DEPARTMENT OF MECHANICAL ENGINEERING

Numerical modelling and dynamic analysis of rocking rigid blocks

Sokratis Anagnostopoulos
Supervisor: James Norman

Report Submitted for the Degree of Engineering June 2017

Acknowledgements

I would like to express my sincere gratefulness to all the people that enhanced my attempts in the production of the present dissertation, starting from my supervisor, Dr James Norman, who believed in my abilities when he gave me this project and was keeping me on the right track on a weekly basis. I would also like to thank Dr Nicholas Alexander and Professor George Mylonakis for their useful ideas and feedback, concerning my methods and approach towards the Rocking Blocks problem. Furthermore, I deeply appreciate the aid of Dr Joel Ross, who extensively spared his time when assisting me in the conduction of my experiments and all the Staff of the Earthquake and Geotechnical Laboratory, who allowed me to use all the necessary equipment for an extended amount of time. Finally, I feel truly obliged to express my gratitude for my family, which is my main source of inspiration and who made everything feasible.

DECLARATION

> *The accompanying research project report entitled: "Numerical modelling and dynamic analysis of rocking rigid blocks" is submitted in the third year of study towards an application for the degree of "Bachelor of Engineering" in Mechanical Engineering at the University of Bristol. The report is based upon independent work by the candidate. All contributions from others have been acknowledged above. The supervisors are identified at the start of the report. The views expressed within the report are those of the author and not of the University of Bristol.*

I hereby declare that the above statements are true.

Signed (author)

……..

Full Name

……..

Date

……..

Declaration of Copyright

Certification of ownership of the copyright in a dissertation presented as part of and in accordance with the requirements for the Final Degree of Bachelor of Engineering at the University of Bristol, Faculty of Engineering.

I hereby assert that I own exclusive copyright in the item named below. I give permission to the University of Bristol Library to add this item to its stock and to make it available for consultation in the library, and for inter-library lending for use in another library. It may be copied in full or in part for any bone fide library or research worker on the understanding that users are made aware of their obligations under the copyright legislation, i.e. that no quotation and no information derived from it may be published without the author's prior consent.

Author	
Title	
Date of Submission	

Signed (author)

……..

Full Name

……..

Date

……..

This dissertation is the property of the University of Bristol Library and may only be used with due regard to the author. Bibliographical references may be noted but no part may be copied for use or quotation in any published work without prior permission of the author. In addition, due acknowledgement for any use must be made.

Summary

The rocking block problem concerns the response of one or more rigid bodies which can rotate and impact on the ground and on top of each other, subjected to gravity or other forces, like seismic waves. Ancient monuments and contemporary free standing or modular structures and artifacts are among the possible applications. This report aims to investigate such single and double block systems behaviour by modelling their dynamic rocking response. To achieve that, a compact mathematical model describing the rotating motion and impacts of a block system was derived, combining effectively all the different cases of possible configurations into a single set of equations. The analytical model was then integrated numerically by a developed computer software, and its validity and accuracy was verified after various self-consistency tests of the algorithm. Moreover, several experiments were conducted in a laboratory set up constructed to test free and forced rocking motion of single and double block configurations. The error margins of the measurements were determined and the extracted data appeared to agree well with the numerical results for most examined cases. To achieve that, the ideal restitution coefficient of a block impact was adjusted to represent real conditions, and was found to be correlated with the block aspect ratio. The integrated model was finally applied to produce normalized overturning maps for a block subjected to single-pulse sine inputs. The forced rocking of a two-block system showed numerically and experimentally that can exhibit numerous different response patterns, depending on the excitation conditions.

Table of Contents

List of Figures

1 Introduction

For centuries, independent rigid blocks have been used as the fundamental structure for various building purposes due to their superiority in construction time, the low cost and the flexibility of use (www.steelconstruction.info/modular_construction). Modular structures in which a large block is placed above a block-like base have been extensively used in Greek and Roman type ancient structures against one-piece buildings, because of their resistance to material failure, as they do not develop high shear stresses under external vibrations (Makris and Vassiliou, 2015). However, structures of unanchored blocks are more prone to tip, which can have catastrophic effects during an earthquake.

From shipping containers, modular construction projects (e.g. rooftop extensions, up to 20 storey buildings, https://triumphmodular.com/wp-content/uploads/2014/09/MBI_Durability_Paper.pdf) and houses in less developed countries, to monuments like Stonehenge and Parthenon, and modern free founded block-structures (oil storage tanks, water towers, computer equipment, and many artefacts) the rocking blocks problem has been a challenge of past and modern mechanics. Nevertheless, while material failure cannot be tamed, the behaviour of a given modular configuration can be modelled, predicted and even optimised. While the empirical methods of our elder engineers have granted us a great cultural heritage, the tools that we have developed today can provide great capabilities of modelling and analysis, which can give us a deeper understanding of the problem.

Several researches investigate the seismic response of classical monuments (columns and other megalithic structures), that are constructed in a modular manner. The dynamics of a single block rocking has intrigued a great number of seismologists and engineers over the years and numerous academic papers have been published. The first simple model for the calculation of the effects of an impact on the rocking motion of a rigid body (energy dissipation and new angular velocity) was derived by Housner (1963), based on the principle of angular momentum conservation. This theoretical model is being used until today, though it refers to idealized impact conditions and blocks geometries. Aslam (1980) studied the rocking and overturning response of various blocks under strong earthquake accelerations, as also the behaviour of vertically pre-stressed blocks to the floor.

Ishiyama (1982) defines a coefficient that determines the horizontal (in addition to vertical) impulse during impact whose effect is mostly neglected in the usual analysis of impact. A computer program to simulate various types of motion and to find criteria for overturning under sinusoidal and earthquake excitations was also used. Papastarnatiou and Psycharis (1993) used piece-wise linear equations, to model the rocking of stone columns, and found the they can predict the overturning, although this model is valid only for small rocking angles. They also found that a modular column behaves like a system of two-blocks, but the number of stones in each of the two blocks depends on the external excitation. Mouzakis et al. (2002) carried out experiments on earthquake response of a model of classical marble column of Parthenon, and found that its response is very sensitive to the initial conditions of the experiments or to any imperfections of the geometry of the blocks. They concluded that their measurements cannot be repeatable, since the same experimental conditions produced different results.

El Gawady et al. (2006) provide experimental results for the rocking response of rigid blocks with aspect ratio 1:5, studying the effect of the interface material, that was found to have significant effect on the rocking behavior of the block. The restitution coefficient obtained by the simple rocking model of Housner was close to the measured one for concrete base, but

much different for rubber base. Baratta and Corbi (2012) describe the pure rocking motion of a unilateral rigid system undergoing a dynamic excitation. The problem of rocking motion is approached in a full distributional context, allowing to set in a unified formulation the equations of the rocking motion. Damping effects were not introduced by means of a coefficient of restitution but acknowledged as a consequence of the of impulsive forces.

In the work of Schau and Johannes (2013), equations of motion and angular momentum conservation at impact for one block are derived to determine restitution coefficient. Numerical solution is done by using the explicit classical fourth-order Runge-Kutta method, with variable time step at impact conditions to increase accuracy. Also, finite element analysis was implemented, to allow the consideration of elastic or plastic properties of the material (especially of the base) and to study the influence of variations from the ideal geometry. Dimitrakopoulos and Dejong (2012) provide closed-form solutions and original similarity laws for better understanding on the fundamental aspects of the rocking block. They also examined the transient dynamics of the rocking block under finite-duration excitations, expressed in appropriate dimensionless groups. Using this formulation, the nonlinear and non-smooth rocking response to pulse-type ground motion can be directly determined, and need only to be scaled by the intensity and frequency of the excitation. The coefficient of restitution is treated as an independent parameter and its influence is analysed. In the work of Voyagaki, Psycharis and Mylonakis (2013), the behaviour of a rectangular block subjected to idealised acceleration pulses was expressed by a generalized function controlled by a single shape parameter. Linearised equations of motion were used, under the assumption of slender block geometry and rocking without slip. Simple overturning criteria for different earthquake waveforms are presented in the form of dimensionless closed-form expressions and graphs that provide insight into the physics of the response.

The work of Makris and Vassiliou (2015) involves the planar rocking response of an array of freestanding columns capped with a freely supported rigid beam (1 DOF problem). A larger size rocking column corresponds to a more stable configuration; therefore, the presence of the freely supported cap-beam renders the rocking frame more stable despite the rise of the centre of gravity. The heavier the freely supported cap-beam is, the more stable is the rocking frame, implying that top-heavy rocking frames are more stable than when they are top-light. The stability of the rocking frame is independent of the number of columns and depends only on the ratio of the weight that is transferred to the column to the weight of the column together with the size and the slenderness of the columns.

In a recent study, Kalliontzis et al. (2017) examined in detail the rocking model of Housner and used past data of free-standing rocking blocks to evaluate its reliability. This model has been reported to consistently underestimate the experimental records with their error difference increasing with decrease in slenderness ratio. In they work, the propose a more realistic model to obtain the restitution coefficient after an impact, assuming that the block rotates with respect to points that are close but not exactly at its bottom corners. Estimates of the locations of these points were obtained experimentally based on new data from free vibration rocking tests of three free-standing concrete members. The article includes tabulated data of experimental values of restitution coefficients measured by various researchers for various block slenderness ratios and block/base materials, along with the corresponding predictions of the Housner's rocking model equation.

One may notice that the complexity of the problem increases exponentially as more blocks are added in the analysis. Thus, while the goals of the literature that deals with a single block lie within a wide spectrum of analysis, the literature that involves two or more blocks mainly aims at deriving an integrated theoretical model. Spanos et al. (2001) derive analytic

expressions involving two blocks for each particular pattern of their combined rocking. This is one of the very few publications that includes a model for the impacts, which is again expressed for each of the many possible combinations of impact points and relative blocks position, along with additional transition conditions from one pattern to another. Such kind of analysis is very difficult to be programmed and checked in a computer code, even if they are perfectly correct, which is not the case in this work: the various expressions contain many errors (typos, wrong signs, even wrong terms). The authors simulate the system by a numerical algorithm and use a 4^{th}-order Runge-Kutta method for time integration. They provide only numerical results for free rocking and for a horizontal earthquake excitation which are not validated with any self-consistency test of the code or experimentally. They also use a simplified system of linearised equations for small rotation angles, but the results deviate significantly from the exact non-linear formulation ones.

Kounadis. et al. (2012), analyse a two-block system under ground motion and compares the stability of the system to that of an equivalent single block. All possible configuration patterns exhibited by the two-rigid block system during rocking motion are modelled and the corresponding mathematical expressions are derived using Lagrange equation and the new angular velocity is simply obtained by assuming a 5% reduction in kinetic energy (no use of angular momentum conservation for impact expressions). The minimum amplitude ground acceleration among all patterns, which leads the system to overturning instability is determined. It is found that for moderately large values of excitation frequencies overturning instability occurs after impact. Beyond these values overturning instability without impact prevails. In case of overturning instability without impact, surprisingly enough, it was also found that there are ranges of values of excitation frequencies in which a monolithic rigid block as a 1-DOF system becomes more stable when divided into two equal rigid blocks, acting as a 2-DOF system.

As the number of blocks increases, the spectrum of the scientific research becomes narrow. From the analytical formulation in the publication of Minafo. et al. (2016), it emerges that despite the method providing a direct physical insight of the problem it can be implemented only for a system with no more than 3 sub-blocks. The case study has shown that multi-block systems for the range of examined parameters are less sensitive to overturning risk with respect to the monolithic member with the same geometrical dimensions, and that overturning conditions depend on the frequency of the external input. The analysis of stacked rigid block systems is made complex as the number of blocks increases, because the number of rocking patterns increases exponentially. The paper uses the Euler-Lagrange method of analysis and integrates numerically the nonlinear equations for 3 blocks, using the Kutta-Merson method. A constant restitution coefficient is used for all impacts, instead of the principle of conservation of angular momentum.

Even though there have been numerous laudable attempts studying the rocking blocks problem, it appears that so far, there hasn't been any integrated model including the equations of motion and impact without the need of additional conditions or conventional assumptions. The present project aims to unify all the governing equations describing the rocking and impact behaviour of a system of up to two rigid blocks, by deriving an analytic model from scratch. A main target was for the model to be as compact as possible so that it could be programmed efficiently. To this aim, a special computer algorithm was developed on Matlab for the numerical modelling of blocks under free and forced rocking motion, and it was used to provide a better understanding of the problem. Also, an experimental study was designed and performed in the laboratory in order to measure the free and forced rocking motion of single and two-block systems and validate the reliability of the predictions.

2 Materials and Methods

2.1 Problem description

The fundamental motion stages that describe the displacement of rectangular rigid bodies (blocks) in space are the following: translation, rotation (rocking), sliding and rest (Shau, 2013). Combinations can also occur where each motion can be described separately.

Rocking block analysis can get very complicated if there is no clear outline of the problem. Thus, several assumptions are usually made for the theoretical analysis of single or combined blocks motion, which are also adopted in the present work:

- The blocks are perfect rectangles.
- The body of the block and the base are rigid.
- There is no bouncing or complete lifting of the body.
- Blocks are assumed not to be sliding on the ground or with each other.
- Material stiffness and damping are not considered. In other words, the blocks cannot be compressed nor store elastic energy.
- Horizontal and vertical vibrations are applied at the centre of mass of the block.
- Energy loss at impact is proportional to a coefficient of restitution (*r*).
- The impact occurs at a single point (point contact), which is a corner of the block.
- The impact lasts for an infinitely small time interval.
- The blocks have the same length.
- The model is simplified for a 2-D geometry since there is no motion on the z-axis.

A typical block-ground system is shown in Figure 1, where the symbols used for each parameter of a single block are depicted and explained. Note that the same symbols will be used for the case of two blocks as well, with the appropriate index denoting the number of the block: 1 for the lower and 2 for the upper block. In that case, the two blocks can have different height and mass.

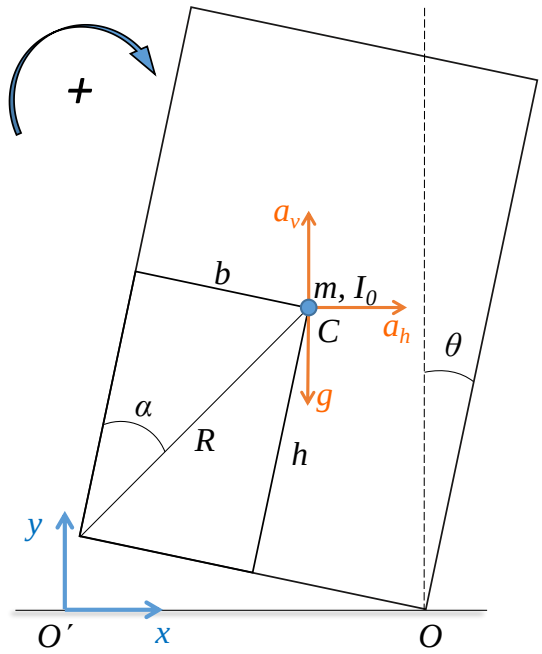

Figure 1: Rocking block sketch.

Symbol	Parameter
a_h	Horizontal seismic acceleration
a_v	Vertical seismic acceleration
b	Half block length
b/h = tan(α)	Aspect ratio
C	Centre of mass
g	Acceleration of gravity
h	Half block height
$I = mR^2/3$	Moment of inertia about C
$I_O = I + mR^2$	Moment of inertia about O/O´
O	Left corner indicator
O´	Right corner indicator
m	Mass
R	Length of half diagonal
α	Critical angle of rotation
θ	Angle of rotation

Table 1. Rocking block parameters.

The rocking motion of a single block can be described by the variation of its angular position, θ, relative to the (horizontal) ground. Clockwise is taken as the positive direction, therefore, the block is at positive angles when it rotates over its right corner (Figure 1), and at negative angles when it stands at its left corner. Also, the holding torque due to gravity is negative or positive, respectively. The position of the block corners and center are calculated in a Cartesian system, the origin of which is at the lower left corner, O′.

In the present work, the motion of a single block or a two-block system is studied at first as free rocking motion, in which the blocks start from an initial non-zero angular position and rotate under the action of gravity. Then, a forced excitation motion is considered, in which the ground can have a horizontal seismic acceleration, a_h (Figure 1). In this case, the calculations are made in the relative Cartesian system, so as the origin remains at point O′. Vertical acceleration can be also applied, by simply adding an extra variable term a_v to g.

2.2 Analytical model of a single block

The derivation of the mathematical analysis is composed of two sections: the motion and the impact equations. Even though the equations of motion describe the behaviour of the block-ground system for most of the time, impact equations are also important because they are controlling the energy dissipation of the block.

2.2.1 Equations of motion

Since this is a dynamic problem, the Euler-Lagrange equation is usually used in multi-block studies to produce a second order differential equation with respect to angle θ of the block (Rajasekaran, 2009). Here it is also used for derivation of the single block motion equations.

$$\frac{d}{dt}\left(\frac{\partial T}{\partial \dot{\theta}_i}\right) - \frac{dT}{d\theta_i} = \frac{dW}{d\theta_i} \tag{1}$$

where T and δW is the kinetic and potential energy of the centre of mass, respectively, and i is the block number, which in this case is one. In order to find the expressions of T and δW, the horizontal and vertical displacements (u_C, v_C) of the centre of mass are required (Figure 2). While rotation occurs around the lower right or left point we can also define the displacements of the upper left/right corners that will be used later for two-blocks modelling:

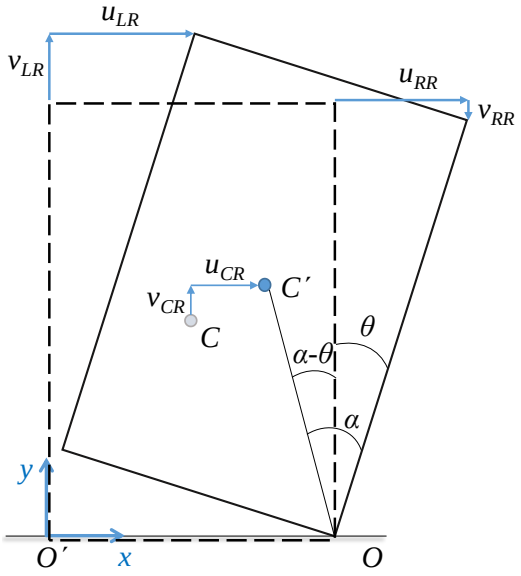

Figure 2: Definition of displacements.

$$u_{LR} = 2R(\sin(a) - \sin(a-\theta)) \tag{2}$$

$$v_{LR} = 2R(\cos(a-\theta) - \cos(a)) \tag{3}$$

$$u_{RR} = 2Rcos(a)\sin(\theta) \tag{4}$$

$$v_{RR} = 2Rcos(a)(\cos(\theta) - 1) \tag{5}$$

$$u_{CR} = \frac{u_{LR}}{2}, \quad v_{CR} = \frac{v_{LR}}{2} \tag{6}$$

where the first subscript denotes the point of interest (upper left or right corner, or center) and the second the corner of rotation (e.g. equation (3) gives the vertical displacement of the upper left corner while the block rotates about the lower right corner). The corresponding expressions for rotation with respect to the lower left corner are given in the Appendix, and show some symmetry (though not exact) in respect to the rotation corner. Hence, a binary indicator was introduced in the present work (C_R), in order to reduce the number of equations and to obtain a single final equation for the motion of the block, regardless the rotation corner.

$$C_R = \begin{cases} 1, & rotation\ around\ right\ corner \\ 0, & rotation\ around\ left\ corner \end{cases} \tag{7}$$

In this way, the algorithm does not have to examine two separate cases, $\theta > 0$ and $\theta < 0$, which is the common practice. This indicator is also used for the case of two blocks, achieving a significant gain in both simplicity and generality of the model,

Thus, the general expression for the displacement of the center of mass becomes:

$$u_C = R[\sin(a) - \sin(\alpha - \theta)]C_R + R[sin(\alpha) - \sin(\alpha + \theta)](1 - C_R) \tag{8}$$

$$v_C = R[\cos(a - \theta) - \cos(\alpha)]C_R + R[\cos(a + \theta) - \cos(\alpha)](1 - C_R) \tag{9}$$

Hence, the expressions for the kinetic and the potential energy of the block will be

$$T = \frac{1}{2} I_o \dot{\theta}^2 \tag{10}$$

$$\delta W = m[a_h u_c + (a_v + g)v_c] \tag{11}$$

By substitution of (10) and (11) into (1) and after some algebra, we finally get the general equation for the rocking motion of a single block

$$\ddot{\theta} = \frac{m}{I_o}[a_h \frac{du_C}{d\theta} + (a_v + g)\frac{dv_C}{d\theta}] \tag{12}$$

where

$$\frac{du_C}{d\theta} = R[C_R cos(a - \theta) + (1 - C_R)\cos(a + \theta)] \tag{13}$$

and

$$\frac{dv_C}{d\theta} = R[C_R sin(a - \theta) - (1 - C_R)\sin(a + \theta)] \tag{14}$$

Note that the term $\frac{dT}{d\theta_i}$ is zero because the expression of T does not have any θ_i terms.

2.2.2 Equations of impact

Under the assumption that the impact happens at a single point (corner) and lasts for an infinitesimal time interval, the angular impulse of the acting forces there can be neglected, and hence the angular momentum of the block about that corner does not change. In this way, the angular velocity of the block just after an impact can be found by applying the conservation of angular momentum, which is defined as

$$h = I\dot{\theta} + \vec{r} \times m \cdot \overrightarrow{V_C} \tag{15}$$

where $\vec{r}$ is the vector from a given point (here the rotation corner) to the centre of mass and $\overrightarrow{V_C}$ is the velocity vector of the centre of mass. Therefore:

$$h_{o'}^{-} = h_{o'}^{+} \quad \rightarrow \quad \left(I + mR^2\sin(\varphi)\right)\dot{\theta}^{-} = (I + mR^2)\dot{\theta}^{+} \tag{16}$$

where φ is $\frac{\pi}{2} - 2a$, as shown in Figure 3.

Thus, the coefficient of restitution after an impact is defined as:

$$r = \frac{\dot{\theta}^{+}}{\dot{\theta}^{-}} = \frac{I+mR^2+\cos(2a)}{I+mR^2} = 1 - \frac{3}{2}\sin^2(a) \tag{17}$$

The above mathematical equation (17) was first derived by Housner (1963) who introduced the model of simple rocking motion of a single block. Using this simple expression, the angular velocity of the block just after an impact, $\dot{\theta}^{+}$, can be obtained from its previous value,$\dot{\theta}^{-}$, depending only on the aspect ratio of the block.

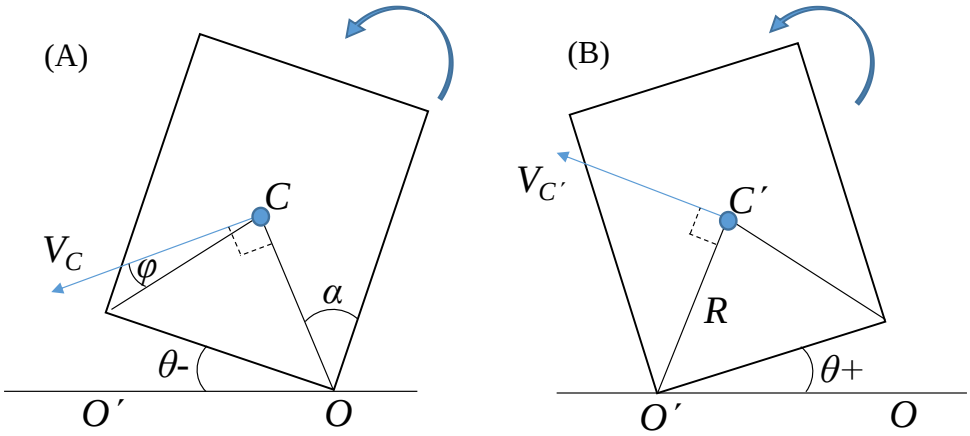

Figure 3: Rocking diagram before (A) and after (B) impact.

The value of the restitution coefficient is less than 1 (e.g. for h/b = 2 it becomes 0.7), therefore there is an amount of kinetic energy dissipated during the impact (eq. 10). In real block systems, the dissipated energy during an impact is mainly transferred to the ground (energy radiation), but can be also spent in inelastic impact or friction mechanisms. However, the assumption of point impact and perfect rectangular geometry leads to an underestimation of *r*, the value of which may be quite higher in practical systems (Schau and Johannes (2013), Dimitrakopoulos and Dejong (2012), Kalliontzis *et al.*, (2017)). This behavior is considered in the present work as will be discussed later.

2.3 Analytical model of two blocks

2.3.1 Equations of motion

The process of mathematical derivation for a system of two rigid blocks is similar with the single block. However, the equations that describe the blocks are now coupled, which requires a system to be solved simultaneously. To create such a system, the expressions of *T* and *δW* can be generalized for *n* blocks. Thus, equations (10) becomes

$$T = \frac{1}{2}\sum_{i=1}^{n} I_{oi}\left(\dot{\theta}_i\right)^2 + \frac{1}{2}\sum_{j=2}^{n} m_j\left[\left(\dot{u}_{T\,j}\right)^2 + \left(\dot{v}_{T\,j}\right)^2\right] \tag{18}$$

where u_{Ti} and v_{Ti} are the cumulative displacement of the centre of mass (Figure 4):

$$u_{T_i} = U_i + u_{Ci} \tag{19}$$

$$v_{T_i} = V_i + v_{Ci} \tag{20}$$

and U_i, V_i the displacement of block i caused by its supporting box (see also Figure 2).

$$U_j = (u_{Rj-1})C_{Rj} + (u_{Lj-1})\big(C_{Rj} - 1\big) + U_{j-1} \tag{21}$$

$$V_j = (u_{Rj-1})C_{Rj} + (u_{Lj-1})\big(C_{Rj} - 1\big) + V_{j-1} \tag{22}$$

and u_{Ci}, v_{Ci} the displacement of centre of mass due to the rotation of the block (eq. 8, 9).

Consequently, the first sum of kinetic energy expression (18) is due to rotation whereas the second is due to translation of a block in respect to its initial rest point, as shown in Figure 4. For n = 2 blocks only U_2 and V_2 are computed, since $U_1 = V_1 = 0$.

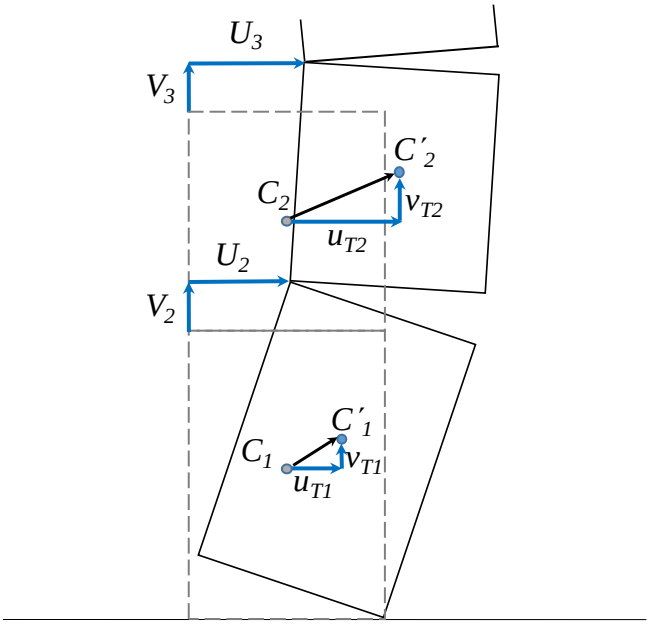

Figure 4: Rocking motion of two blocks.

On the other hand, for n blocks equation (11) for the potential energy becomes:

$$\delta W = \sum_i^n m_i[a_h u_{Ti} + (a_v + g)v_{Ti}] \tag{23}$$

By substituting the partial derivatives of equations (18) and (23) into equation (1), a system of n equations is created. For the present case the system consists of two equations, one being the derivatives with respect to θ_1 and the other to θ_2. Therefore, the system of differential equations describing the rocking motion of two blocks becomes:

$$\begin{cases} \ddot{\theta}_1 = \begin{bmatrix} -m_1\left(u_h\frac{du_{T1}}{d\theta_1}+(g+a_h)\frac{dv_{T1}}{d\theta_1}\right)-m_2\left(u_h\frac{du_{T2}}{d\theta_1}+(g+a_h)\frac{dv_{T2}}{d_1}\right) \\ -2m_2R_2h_1\left(\dot{\theta}_2^2\cdot\sin(\gamma)\cdot C_{Z2}+\ddot{\theta}_2\cos(\gamma)\right) \end{bmatrix}\cdot\frac{1}{I_{O1}+m_2.c} \\ \ddot{\theta}_2 = \begin{bmatrix} -m_1\left(u_h\frac{du_{T1}}{d\theta_2}+(g+a_h)\frac{dv_{T1}}{d\theta_2}\right)-m_2\left(u_h\frac{du_{T2}}{d\theta_2}+(g+a_h)\frac{dv_{T2}}{d\theta_2}\right) \\ -2m_2R_2h_1\left(\ddot{\theta}_1\cdot\cos(\gamma)-\dot{\theta}_1^2\cdot\sin(\gamma)\cdot C_{Z2}\right) \end{bmatrix}\cdot\frac{1}{I_{O2}} \end{cases} \quad (24)$$

where

$$c = 4R_1^2|C_{R1}-C_{R2}|+4h_1^2(1-|C_{R1}-C_{R2}|) \quad (25)$$

$$\gamma = (a_2+\theta_1-\theta_2) \quad (26)$$

$$C_{Z2} = 2\cdot CR_2-1 = \begin{cases} 1, & rotation\ around\ right\ corner \\ -1, & rotation\ around\ left\ corner \end{cases} \quad (27)$$

Note that the explicit expressions of all the differential terms are given in the Appendix.

2.3.2 Equations of impact

The derivation of the new angular velocities of the blocks after an impact ($\dot{\theta}_1^+, \dot{\theta}_2^+$), is based on the same principles as in section 2.2.2. However two critical differences can be noticed: An impact may occur between two different sets of rigid bodies, ground-lower block or upper block-lower block, while the impacts for the latter occur at a variable rotation angle. Thus, a separate system of two equations need to be derived and solved for each impact case, in order to compute the new angular velocities from the conditions just before the impact. To create such systems, the conservation of angular momentum was applied twice for each case.

Impact between lower block and the ground

Let the impact occur at point O′ and the upper block rotating around K, as shown in Figure 5A. The two independent expressions that can be used are the conservation of angular momentum of the upper block alone with respect to K, and of the two-block system with respect to O′. For the lower block just before and just after the impact we have (Figure 5A):

$$h_{O'1}^- = I_1\dot{\theta}_1^- + m_1 R_1^2\cos(2a_1)\dot{\theta}_1^- \quad (28)$$

$$h_{O'1}^+ = I_1\dot{\theta}_1^+ + m_1 R_1^2\dot{\theta}_1^+ \quad (29)$$

while for the upper block the expression is the same (but the velocities before and after the impact are different):

$$h_{O'2} = I_2\dot{\theta}_2 + m_2\vec{d}_2\times\vec{V}_{C2} \quad (30)$$

Also, for the upper block with respect to K there is a single expression, in which again the velocities before and after the impact are different (Figure 5A).

$$h_{K2} = I_2\dot{\theta}_2 + m_2 R_2^2\dot{\theta}_2 + m_2\vec{R}_2\times\vec{V}_K \quad (31)$$

After deriving and analysing the terms of all the above angular momentum quantities, the angular momentum conservation equations take the form of a set of two linear equations:

$$\begin{cases} h_{K2}^{-} = h_{K2}^{+} \\ h_{O'1}^{-} + h_{O'2}^{-} = h_{O'1}^{+} + h_{O'2}^{+} \end{cases} \xrightarrow{yields} \begin{cases} A_1\dot{\theta}_1^{+} + B_1\dot{\theta}_2^{+} = C_1 \\ A_2\dot{\theta}_1^{+} + B_2\dot{\theta}_2^{+} = C_2 \end{cases} \tag{32}$$

The analytic expressions of the coefficients A_1, B_1, C_1, A_2, B_2 and C_2 of system (32) are given in the Appendix. The same equations apply when the impact occurs at the other corner point, O, or when the upper box rotates about its left corner.

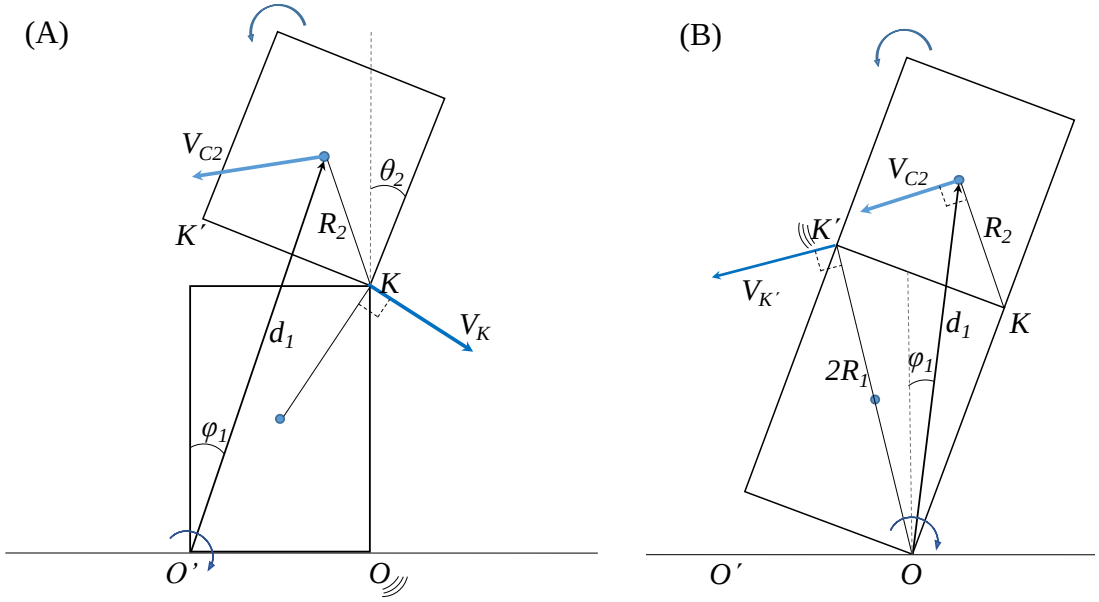

Figure 5: Two-block system impacts: (A) to the ground at the right corner O, and (B) between blocks at point K′.

Impact between blocks

The governing equations for the second case were derived under similar process and produced a similar linear system (32). As shown in Figure 5B, the conservation of momentum for the upper block was applied about the point of impact (K′), whereas for the system of blocks it was applied with respect to O. Hence, the expressions of the various angular momentum terms are different (though similar with the previous). For the upper block, just before the impact at point K′ the angular momentum is (Figure 5B):

$$h_{K'2}^{-} = I_2\dot{\theta}_2^{-} + m_2\, R_2^2 \cos(2a_2)\dot{\theta}_2^{-} + m_2\, \vec{R}_2 \times \vec{V}_{K'} \tag{33}$$

and just after the impact:

$$h_{K'2}^{+} = I_2\dot{\theta}_2^{+} + m_2\, R_2^2\, \dot{\theta}_2^{+} + m_2\, \vec{R}_2 \times \vec{V}_{K'} \tag{34}$$

Also, the expressions for blocks 1 and 2 with respect to point O are:

$$h_{O1} = I_1\dot{\theta}_1 + m_1\, R_1^2\, \dot{\theta}_1 \tag{35}$$

$$h_{O2} = I_2\dot{\theta}_2 + m_2\, \vec{d}_2 \times \vec{V}_{C2} \tag{36}$$

The derived analytic expressions for the coefficients of the final linear system are given in the Appendix. Similar equations apply when the impact is at point K or if the lower block rotates about O′.

2.4 Numerical analysis

The non-linear, second order differential equation (12) for single block, or the system of equations (24) for the two-block system do not have analytic solution and hence they must be solved by a numerical method. Linearisation of these equations for small rocking angles is possible, but the obtained analytic solutions were found to deviate considerably from the correct results (Spanos et al. 2001). In order to be numerically solved, a second-order dif. equations can be decomposed into a system of 2 ordinary differential equations as follows:

$$\frac{d\theta}{dt} = \dot{\theta} = \omega \tag{37}$$

$$\frac{d\omega}{dt} = \ddot{\theta} \tag{38}$$

where $\ddot{\theta}$ is taken from eqs. (12) or (24), and ω is auxiliary variable equal to angular velocity.

The system of the above equations was solved on Matlab using 4th order Runge-Kutta, after it was proven to converge faster than the 1st order Euler method and the Runge-Kutta 2nd order method. To do that, an 'accurate' solution was calculated at first, using a very small time step of 10^{-7} s, with which all methods produced the same results for a free rocking of a block with aspect ratio 1:2, released from an initial angle of +10^{o}. Then, the capability of each method to reproduce this rocking performance was tested using progressively increased time steps. An example of this procedure is shown in Figure 6A for a time step of 0.05 s. For this step Euler method gives quite different results, whereas RK4 follows the correct curve at least for the first impacts (when θ=0).

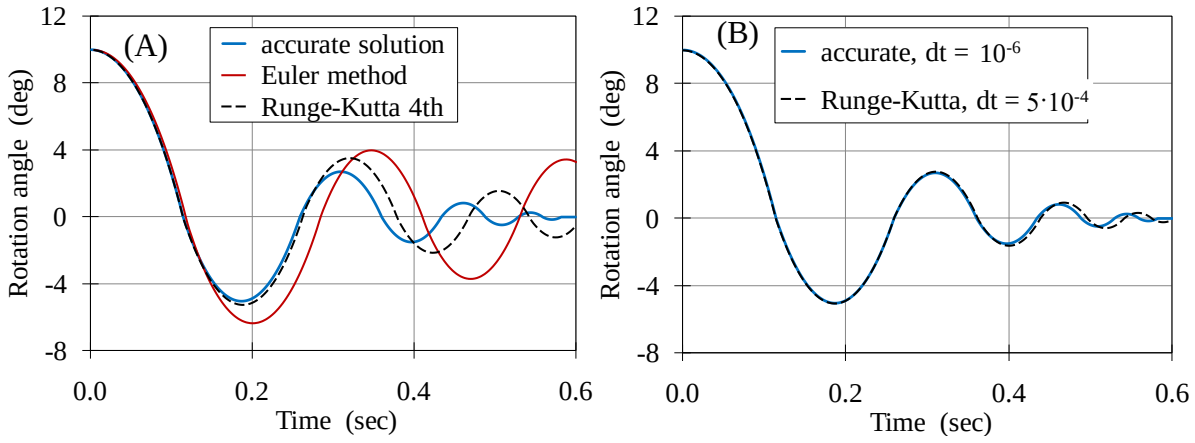

Figure 6: Comparison of results accuracy using different numerical methods (A) and different integration time step (B).

The time step independence was then investigated and the results of RK4 method were found to be almost identical with the accurate solution using a time step of 5x10^{-4} s, as shown in Figure 6B. Consequently, a five-times smaller time step of 10^{-4} sec is considered adequate to produce always accurate numerical results, and this is used throughout the entire study.

In addition to the numerical integration, the developed computer code checks if the impact conditions are met at each time step (impact with the ground or between blocks). In such case, it finds the restitution coefficient from eq. (17) for the single block problem, or calculates the coefficients and solves the linear system (32) for the two-block problem, in order to find the angular velocity of the block(s) just after the impact. This is then taken as new initial condition to continue the integration of the rocking motion equations. For two-

blocks there are 4 coupled differential equations that are solved simultaneously by the RK4 method, which is especially programmed in the computer algorithm for that purpose.

It is worth mentioning that without any special condition, the graphs of Figure 6 would not stop to oscillate around x-axis. Instead, after a minimum amplitude was reached, the oscillations would persist due to the computational accuracy of the computer. A reasonable way to introduce a termination criterion would be to stop the the computations when $\dot{\theta} < \varepsilon$, where ε is a small fraction (here 0.1) of the maximum $\dot{\theta}$ recorded at the previous impacts. This criterion was tested in various cases and found to perform satisfactory, namely to terminate the algorithm when the oscillations of the block become minor. The CPU time required for a complete evaluation of a rocking case by the developed software is very small, and for the present studies it takes a few seconds on a regular computer.

2.5 Experimental set up

Free rocking motion after initial displacement

To confirm the reliability and accuracy of the theoretical expressions and numerical results, several experiments have been conducted with steel rectangular blocks of different sizes (Figures 7 and 8). Using the camera of an iPhone 5S and the application SloPro, which provides slow motion recordings of up to 100 frames per second, the free rocking motion of the blocks was recorded after an initial angular displacement. Thereafter, the angles at which the angular velocity becomes zero (namely at the top oscillation points of the block, where the accuracy of measurement maximizes) were tabulated, along with the corresponding time instant at which they occurred, using a virtual on-screen protractor, as shown in Figure 7.

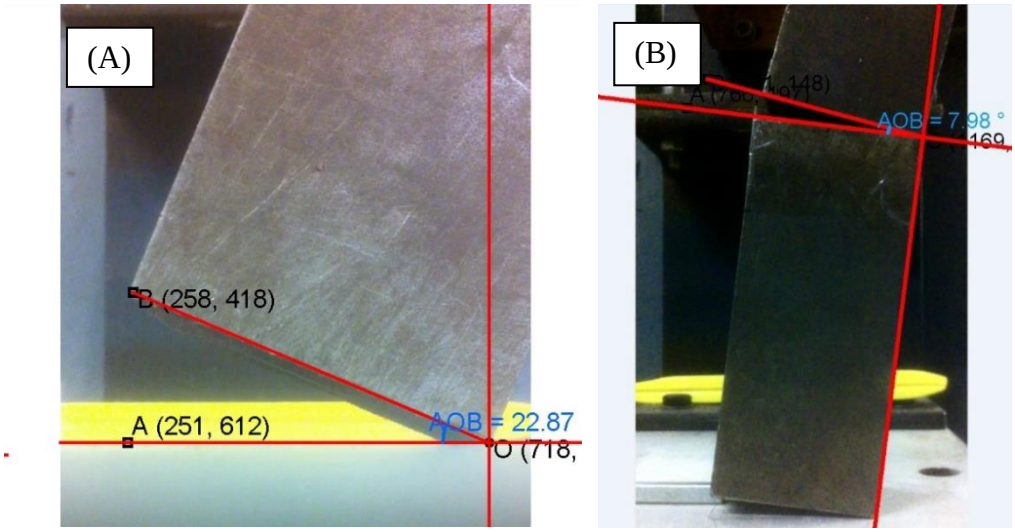

Figure 7: Snapshots from experimental recordings of single (A) and double block free rocking (B).

In an attempt to approximate as much as possible, the ideal conditions of the theoretical analysis, the experiments were conducted under specifications that verged on the initial assumptions. Thus, to maximise the validity of the experiments and minimise the unknowns of the environment, the following measures were taken

- The horizontal levelling of the experimental base surface was tested by a spirit level.
- The selected material of the ground surface had a high modulus of elasticity.
- Each block was selected for having sharp edges to ensure point impact.
- Sliding was prevented using aluminium oxide sandpaper on the surfaces of contact.

- The camera lens was placed on the same level as the examined surface of the block.
- A small item supporting the block at an initial angular position was instantaneously removed to initiate rocking. To ensure that no energy was given to the system, the initial angle of each block was its critical angle. In that way, if a small amount of energy was given to the system at the support removal, the block would tip over.
- To estimate the error margin, several videos were recorded for each case.

Forced rocking motion

In addition to the free rocking experiments, the forced rocking motion of single and two-block systems caused by horizontal vibrations is also investigated in the laboratory. To create such external excitation, a shaking table for academic purposes was used in the earthquake laboratory (Figure 8). Several forced rocking videos were recorded under sinusoidal vibrations with amplitudes of 1.5, 3, 4 and 5 mm. Each time, the frequency was gradually increased up to a point where the angular displacements could be easily measured. The previously stated measures for single block experiments were also taken for the two-block system. Additionally, some extra measures had to be taken for the new configuration in order to ensure the credibility of the recorded data, as shown in Figure 8:

- The shaking table was fixed to the ground using bolt connections.
- The recording device was fixed on the shaking table to measure the displacements of the blocks relative to the table.
- A wooden block was used to support the smart-phone so that the camera lied on the same plane as the block side of interest.
- Any additional shaking of the supporting block and the recording device relative to the table was minimised with the use of double sided tape and super glue.
- To avoid sliding the use of sand paper was not enough. Thus, small pieces of flexible plastic were also placed at block sides perpendicular to the areas of contact.
- A ruler made from hard plastic was often fixed on the table to prevent blocks from sliding back and forth due to the impacts.
- A white background was placed behind the blocks to increase the contrast with the darker blocks and facilitate the angle measurements on the recordings.
- The two blocks had the same area of contact.

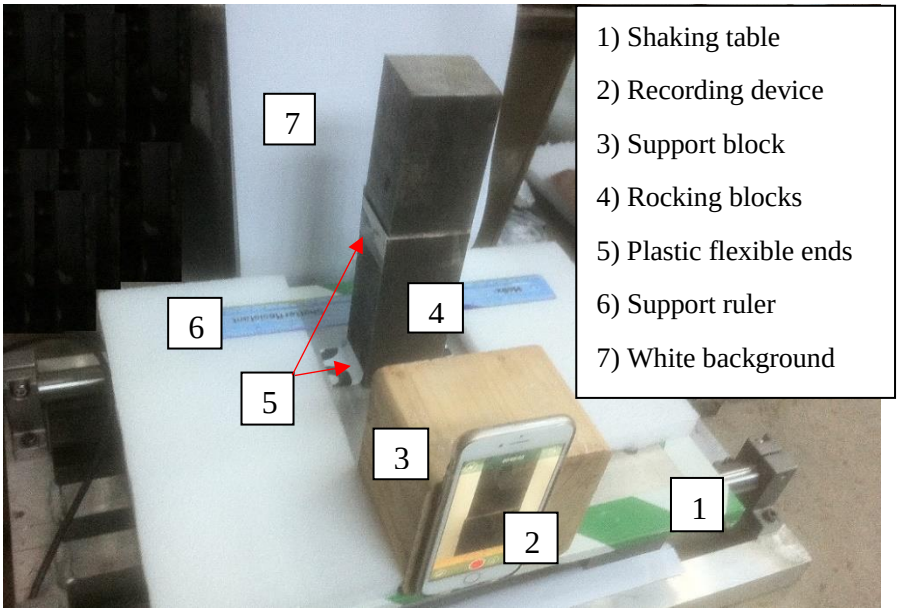

Figure 8: Shaking table apparatus.

3 Results

This section presents and describes various numerical and experimental results obtained in this study to demonstrate the rocking behaviour of single and two-block systems. Discussion and comparative assessment of these results is made in the next section 4.

3.1 Single block analysis

3.1.1 Rocking response

The developed computer code provides plots with the variation of $\theta, \dot{\theta}, \ddot{\theta}$, a_h and a_v, as well as an animation of the simulated motion of the block. Such plots are indicatively drawn in Figure 9, for a free rocking block. It can be seen that the block follows a periodic pattern where both the amplitude and the period are damped. However, judging from Figure 9, the function of the angle cannot be characterised as any of the basic trigonometric, since its derivative, $\dot{\theta}$ develops sharp edges at impacts. Furthermore, the angular acceleration follows the damped oscillation of the angle and develops discontinuities at impacts (Figure 9C).

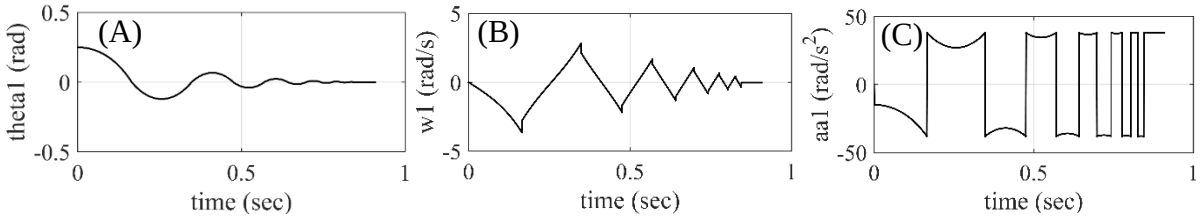

Figure 9: Variation of angle (A), angular velocity (B) and acceleration (C), of a free rocking block.

In contradiction with the patterned results of Figure 10, when external sinusoidal accelerations, a_h and a_v, are introduced (ground excitation) the variation of $\theta, \dot{\theta}, \ddot{\theta}$ becomes more complex and sometimes chaotic, as shown in Figure 10. Yet, the sharp edges of $\dot{\theta}$ at impact are still visible, causing the discontinuities in the graph of the angular acceleration.

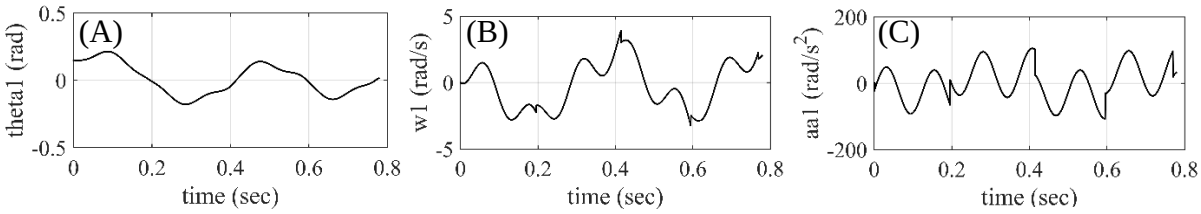

Figure 10: Chaotic responses of a single block under sinusoidal acceleration input.

3.1.2 Experimental and numerical results

The dimensions and mass of each block as measured in the laboratory are tabulated below.

	Dimensions (mm): height x length x depth	Mass (kg)	Aspect ratio (b/h)
Block 1	120 x 29 x 45	1.3	0.2417
Block 2	135 x 60 x 50	2.95	0.4445
Block 3	238 x 60 x 50	5.3	0.2521
Block 4	100 x 60 x 50	2.3	0.6

Table 2. Block properties.

Since this is a 2-D problem, the dimension perpendicular to the plane of rotation is not affecting the motion of the block. Thus, the depth was used only for the mass calculation.

Figure 11 includes numerical and experimental results for the free rocking of Block 2, starting from angular position of +22°. Three different sets of measurements are included in this figure to demonstrate and estimate the experimental errors. This will be discussed in the next section 4, along with the comparison between measurements and numerical results.

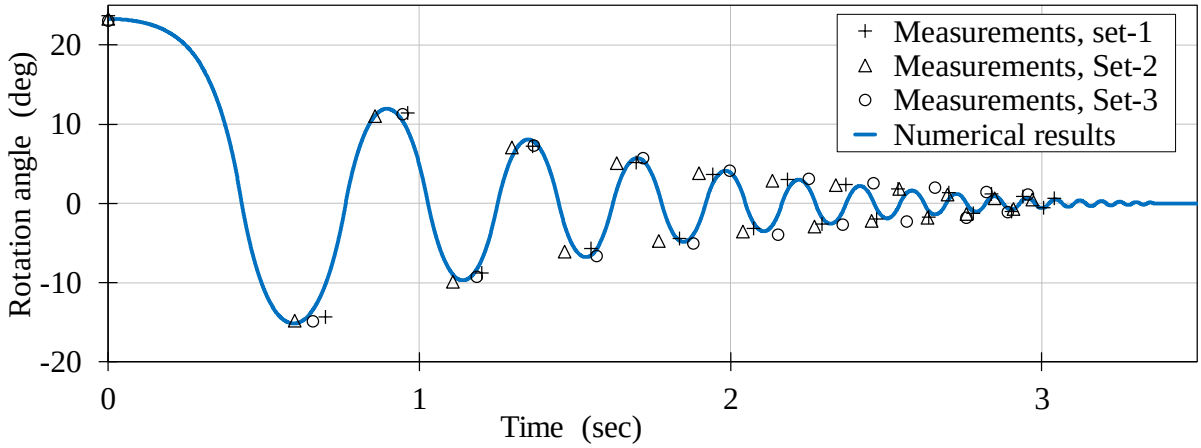

Figure 11: Comparison of experimental and numerical results for Block 2.

Similar experiments were performed under the same assumptions for blocks 1 and 3 (Table 2) and the results are shown in Figure 12. The behaviour of the rocking blocks is similar, but the decay rate of the amplitude and period differs, although they have about the same aspect ratio and initial angular position, because it depends on the absolute size of the blocks (faster decay for smaller block 1 in Fig. 12A).

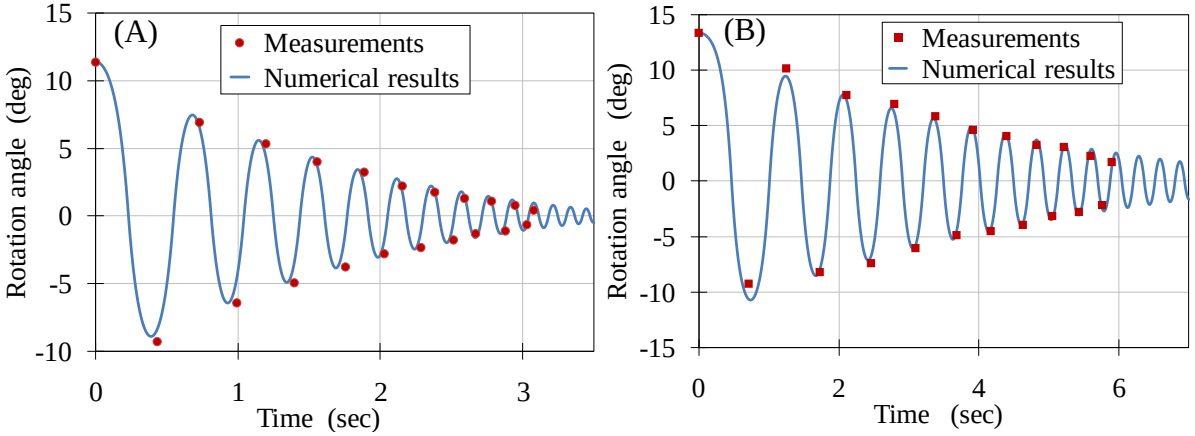

Figure 12: Comparison between experimental and numerical results for block 1 (A) and 3 (B).

Concerning forced rocking conditions, the experimental measurements of Figure 13 are for Block 2 subjected to an external vibration with frequency of 5 Hz and amplitude of 3 mm, after it has reached a periodic motion. In practice, the block performs a chaotic motion until it reaches the harmonic state, as it was also confirmed by the numerical results of the time interval from 0 to 3 seconds in Figure 13.

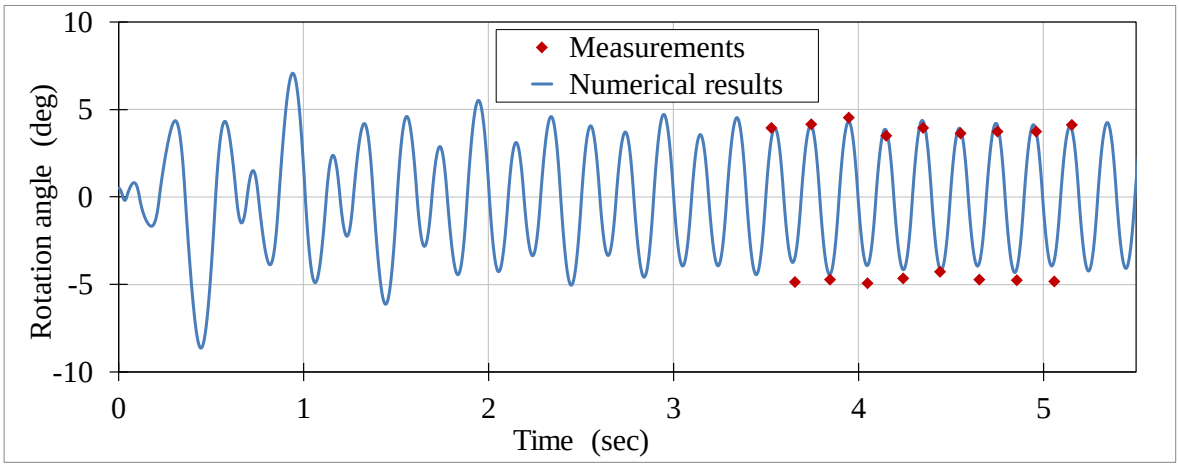

Figure 13: Experimental and numerical results for block 2 under sinus excitation.

3.2 Two-block system analysis

3.2.1 Numerical rocking response

To verify that the code was self-consistent, various symmetry tests were performed, at first for single block free rocking and then for the most complex combined motion of two blocks. In the latter the angle variation with time was recorded after an initial angular displacement of the blocks and repeated for symmetric initial position of the blocks, as shown in Figure 14A. For this particular case the blocks start with opposite initial angles, and perform chaotic rocking motion with impacts to the ground (angle = 0) and among them (intersection points), for about 0.55 seconds. Then, they collide and behave as a single block.

As it is evident from Figure 14B, the angle variation curves of the second test with opposite initial displacement of the blocks were perfectly symmetric, and this is also valid for the precise quantitatively results, thus confirming the correctness of both the derived mathematical model and its incorporation into the computer algorithm.

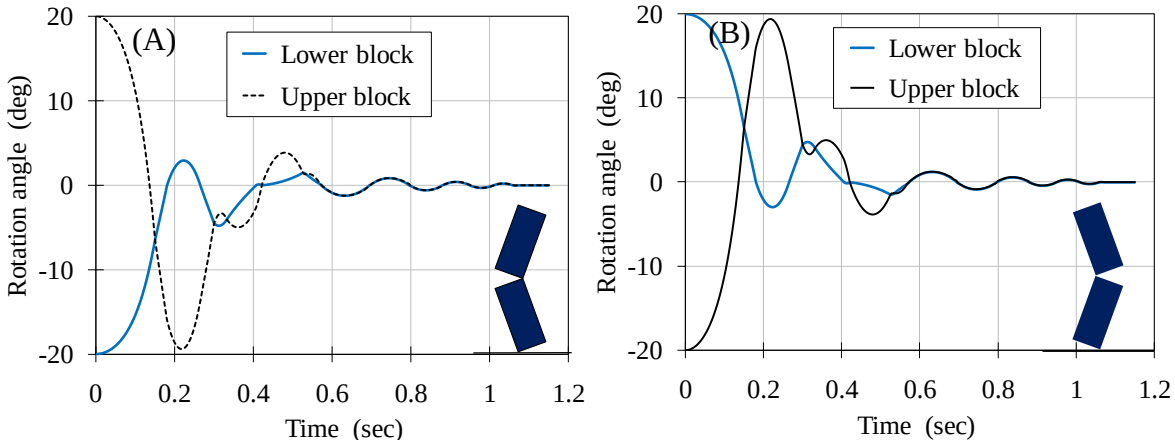

Figure 14: Numerical model self-consistency test for opposite block configurations.

Additional check of the correctness and accuracy of numerical results was carried out using a configuration of blocks with same direction of initial angular displacement (Figure 15). In this case, the lower block moves upwards until the blocks collide to each other. Almost after this first impact, followed by a few small rockings of the upper block on top of the lower, the

two blocks are stick together and continue to rotate as a single box. The resulting rocking curves for anti-symmetric initial position of blocks were again exactly symmetric (Fig. 15).

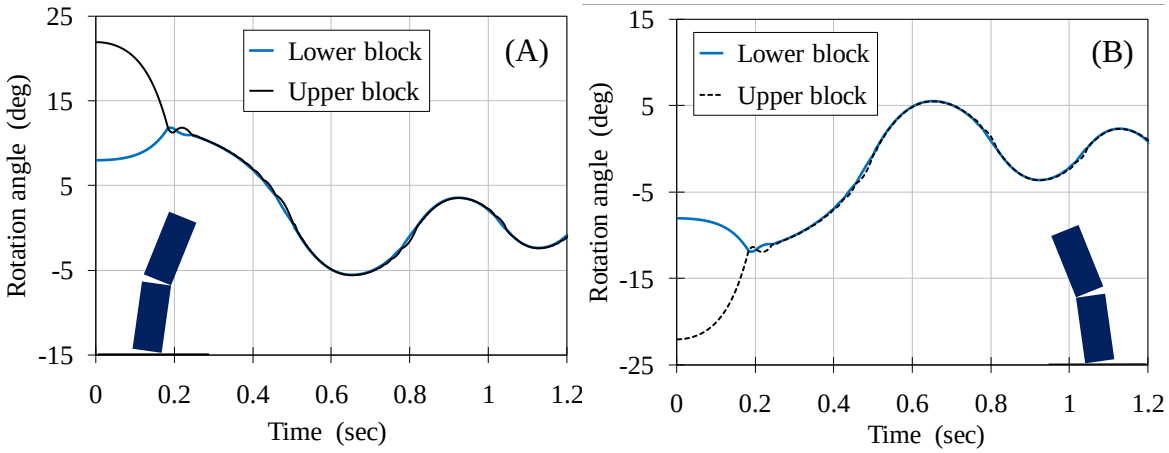

Figure 15: Model self-consistency test for two anti-symmetric block configurations.

3.2.2 Experimental and numerical results

In Figure 16A, two sets of measurements are compared with the numerical results of the angle variation obtained from the algorithm for Blocks 1 (lower) and 4 (upper). In Figure 16B the restitution coefficients in the numerical model were adjusted in order to match the numerical results with the measurements, as will be discussed in Section 4.

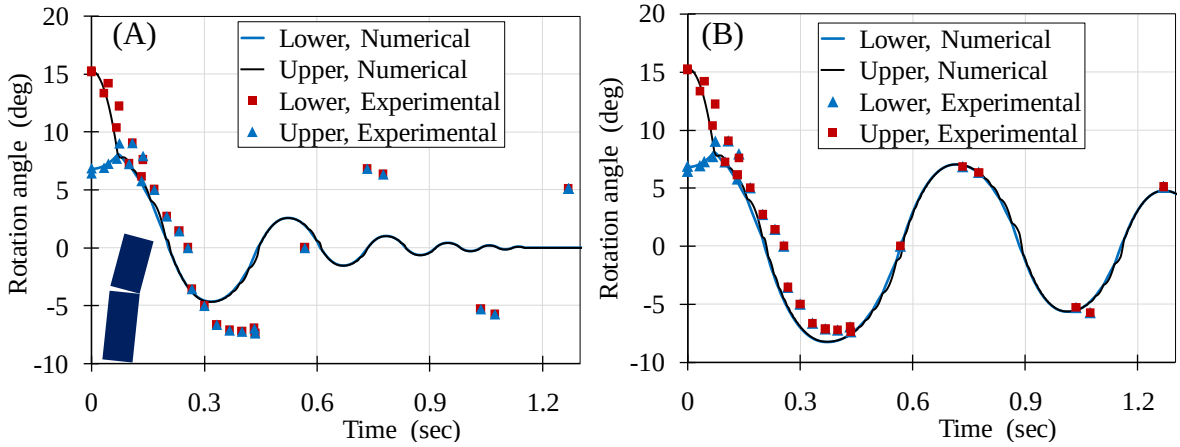

Figure 16: Comparison of two-blocks rocking measurements and numerical results obtained by: A) the present impact model, and B) adjusted restitution coefficients.

Using the same block configuration of Figure 16, various forced rocking experiments and numerical simulations were performed for several different combinations of amplitude and frequency of a horizontal sinusoidal excitation. Some indicative results are shown in Figure 17, revealing the great complexity and diversity of the two blocks system response to external acceleration forces, as will be discussed in the next section.

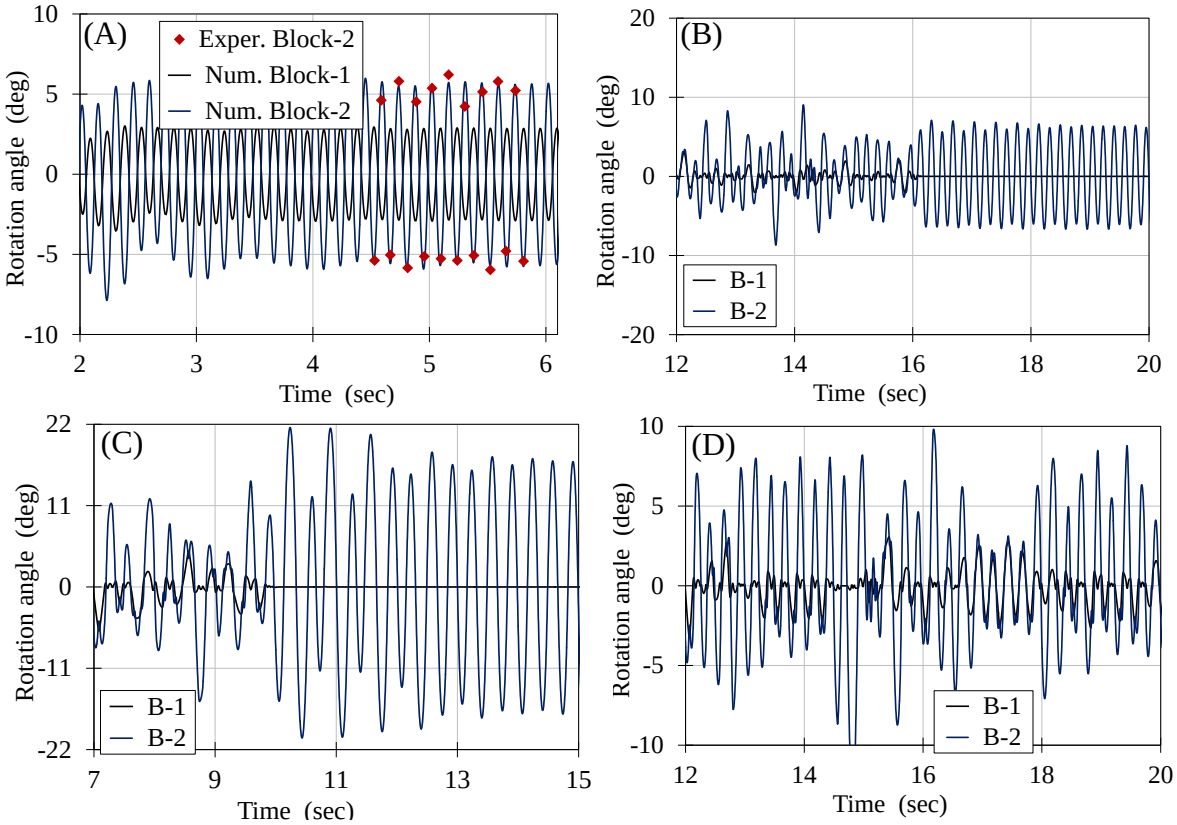

Figure 17: Various motives of two-block rocking forced by external excitations.

3.3 Single block overturning study

The numerical algorithm was used to simulate the overturning behavior of a single rigid block, subjected to a single sinus acceleration pulse in horizontal direction:

$$a_h = a_g \sin(\omega_g t) \tag{39}$$

where a_g is the amplitude and ω_g the angular frequency of the pulse. The resulting overturning maps are presented in normalized form in Figure 17A with the corrected restitution coefficient, taken from Fig. 19 for a block with aspect ratio 1:2 used in the simulations. The frequency parameter p is:

$$p = \left(\frac{3g}{4R}\right)^{0.5} \tag{40}$$

Figure 18B shows the same map with the simple restitution equation (17). The maps are divided in three regions: region 1 represents the stable decaying rocking of the block (or being at rest) after the excitation pulse. In the conditions of region 2 the block overturns after making one impact to the ground, and in region 3 it overturns without previous impact. These regions are clearly bounded in the map, and region 3 is practically the same for both restitution models. However, Housner's model predicts a larger stable region than that with the corrected and more realistic restitution.

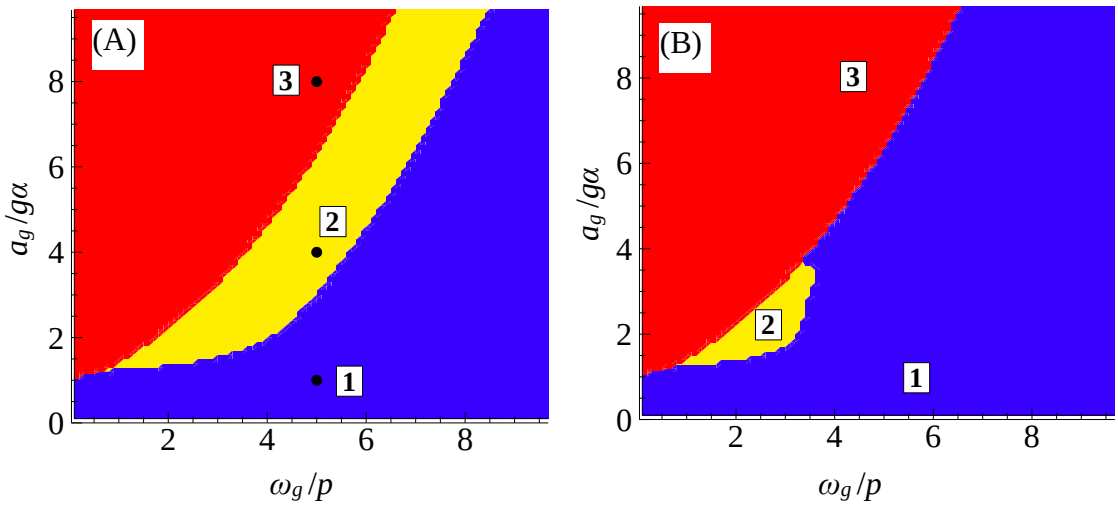

Figure 18: Overturning maps for rocking block subjected to single sinus pulse.

4 Discussion

4.1 Problem analysis and simulation

As shown in Figure 14 and 15, the computer algorithm underwent successfully the self-consistency tests, in order to verify the correctness and accuracy of the numerical results. Similar testing is not reported in the literature, especially for the complex case of two or multiple blocks.

It is worth mentioning that to achieve such performance of the algorithm, the theoretical model underwent numerous iterative error identification processes until all the equations were correct. This process became even more tedious especially for the impact equations, since no published academic paper including the correct expressions was found. Consequently, the debugging process of the numerical model was extremely time-consuming as well. The theoretical error-sweeps and the numerical debugging were often performed in parallel to each other. The self-consistency tests would not give the desirable symmetric results until the very last correction of a single sign.

However, the final product of the approach introduced in the present study, using the binary indicators C_{R1} and C_{R2}, resulted in an analytic model which requires less than 20 lines of code to be programmed for the blocks motion and about 10 lines for each of the two impact cases of a double block system (see Appendix). This is a major advantage compared to the approach of other researchers (e.g. Spanos et. al., 2001), where the large number of mathematical expressions would make the debugging of the algorithm very difficult, since the output is very sensitive to even the smallest mathematical error.

Furthermore, the present approach does not need additional mathematical expressions to model transition from one pattern to another, neither any constraint for the imposed momentum to start rocking motion. It was found that the derived model is capable to produce any dynamic behaviour of the block system. Moreover, the present approach increases significantly the speed of the algorithm, since it eliminates the control commands that would be needed to separate several possible combinations of blocks' rotation and impact points.

4.2 Estimation of the experimental error

Based on the repeated experimental data sets shown in Figure 11, the accuracy of the measured block rotation angle lies within ±0.5º. The error in time measurements can also be extracted from this diagram, since it is only affected by the frame rate of recording. As can be observed, the average time error is of the order of 0.1 seconds, as the difference in time between same measured points of different sets varies between 0.05 and 0.15 seconds. The time error can become significant because whenever the block reaches maximum angular displacement the angular velocity becomes zero. Thus, the exact frame at which the block appeared to be at its maximum displacement could not always be precisely determined.

Another source of experimental error may be the block weight and dimensions measurements, which are affected by the accuracy of the equipment used. All the weight measurements of the blocks were made with an electronic scale of ±0.025 kg accuracy, while the dimensions of each block were measured using a ruler of ±1 mm accuracy. With that error in the length measurement, the error for the critical angle (α) is ±0.6º. Since all the absolute errors are specified, they can be combined to determine a total absolute error in the calculation of $\ddot{\theta}$. For the case of free rocking motion equation (11) is simplified as follows:

$$\ddot{\theta} = \frac{4}{3R}[g\sin(\alpha - \theta)] \tag{41}$$

Evidently, from equation (11) it emerges that the motion of a single block is independent of its mass and thus, it will be neglected in the error calculation. This can be explained by the fact that the angular velocity of the block is only affected by the gravitational acceleration (which is always constant) and the distance of the centre of mass from the point of rotation (R). Therefore, the expression of the absolute error for a function with more than one independent variable can be derived from a multivariable version of the Taylor series (Steven C. Chapra, Raymond P. Canale, 1998) and give the following relationship:

$$\Delta f(\tilde{x}_1, \tilde{x}_2, \dots, \tilde{x}_n) \cong \left|\frac{\partial f}{\partial x_1}\right| \Delta\tilde{x}_1 + \left|\frac{\partial f}{\partial x_2}\right| \Delta\tilde{x}_2 + \dots + \left|\frac{\partial f}{\partial x_n}\right| \Delta\tilde{x}_n \quad (42)$$

where n is the number of the independent variables, $\tilde{x}_1, \tilde{x}_2, \dots, \tilde{x}_n$ which have absolute errors $\Delta\tilde{x}_1, \Delta\tilde{x}_2, \dots, \Delta\tilde{x}_n$ respectively. For equation (11), n=3, $\tilde{x}_1$=R, $\tilde{x}_2$=α and $\tilde{x}_3$=θ.

Thus, from equation (12) it emerges that the absolute error for $\ddot{\theta}$ is ±1.4 rad/s^2 and hence the relative experimental error with respect to acceleration of gravity was estimated to be within ±14%. This is about the same order of magnitude of the experimental error stated by other researchers, who observed that identical experiments may produce quite different results, which are very sensitive to the initial conditions or minor perturbations. For example, the measurements of ElGawady et al. (2006), Kalliontzis et al. (2017) were found to be repeatable with scattering while the measurements Mouzakis et al. (2002) were practically non-repeatable.

4.3 Comparison between measurement and numerical results for single block

The agreement between the present numerical and experimental results shown in Figures 11 and 12 is quite satisfactory. The damping rate of both the amplitude and the period of block oscillation are well comparable. However, to achieve that, the coefficient of restitution taken by equation (17) had to be increased appropriately. According to several previous studies (Kalliotzis et al., 2017), this theoretical model does not represent a realistic scenario because it does not fulfil several of the initial assumptions. Since the blocks are not ideal, the side of contact will always have a small curvature and the impact may not occur at the corner point of the block. In their work, Schau and Johannes (2013) showed that even a very small deviation from the ideal straight line results in remarkably higher values for the coefficient of restitution than predicted by the model.

The values for this coefficient as obtained from equation (17) and as corrected here are tabulated in Table 3 below. For the aspect ratio of the blocks used here, and for similar block/base materials, the obtained correction factors in Table 3 are close to the ones suggested in the work of Kalliontzis et al. (2017). Moreover, Figure 18 shows that the correction factor can be correlated with the critical angle (or the aspect ratio) of the blocks, though more data are needed to extract a safe conclusion. However, it appears that the required correction factor increases with the critical angle of the block.

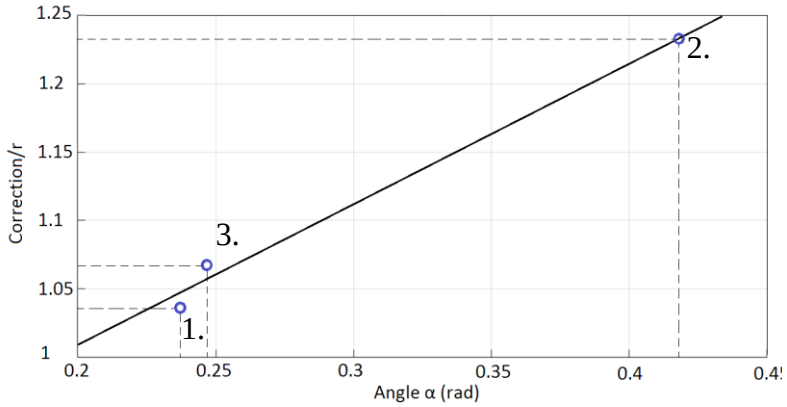

Figure 19: Relationship between the critical angle and the ratio of the correction in r over the values obtained from equation (16).

Block	r (eq. 16)	Correct. factor	New r
1	0.9172	1.036	0.950
2	0.7527	1.233	0.928
3	0.9104	1.067	0.971

Table 3. Original and corrected coefficient of restitution with their corresponding factor

Concerning the forced excitation case, the comparison between experiments and calculations shown in Fig. 13 is again satisfactory. However, as can be observed in the measurements, there is a small divergence in the amplitudes of one side of rotation. This could be attributed to the systematic error of the transfer function of the table controller, which results in a non-symmetric amplitude output of the shaking table. The numerical algorithm predicts the time intervals between each peak successfully.

4.4 Two blocks simulation and experimental results

From the comparative results of Fig. 16A it appears that the experimental points show a remarkable discrepancy from the output of the algorithm, especially after the collision of the blocks. Nonetheless, this was expected due to the overestimation of the coefficient of restitution analysed above. Thus, it became apparent that the use of a correction factor was again necessary in order to match the experimental results with the ones obtained by the model. In this case however, such correction is not easy, because it affects the behaviour and the kinetic energy of both blocks, especially when after the first impacts the two blocks continue to move together.

As it can be observed in Figure 20, which represents an enlargement detail of Figure 15A, the angle variation of the upper and lower block is never identical, as many microscopic impacts constantly occur. In fact, for the duration of 0.24 to 0.55 seconds shown in Figure 19, the blocks collided for as many as 30 times. Even though these results need to be verified experimentally as well, it becomes apparent that there is no need for a special condition for keeping the blocks united. On the other hand, the dissipated kinetic energy at each impact as predicted by the conservation of momentum model, causes additional reduction of the system kinetic energy and faster damping. But due to the large number of impacts, this restitution is not controllable and even small fixed correction factors may destabilise the system or produce unrealistic results.

For this reason, a constant restitution coefficient is adopted for this case, the value of which was adjusted in order to improve the agreement of the numerical results with the measurements shown in Figure 16B (0.95 for the ground impact and 0.98 for the small impacts between blocks).

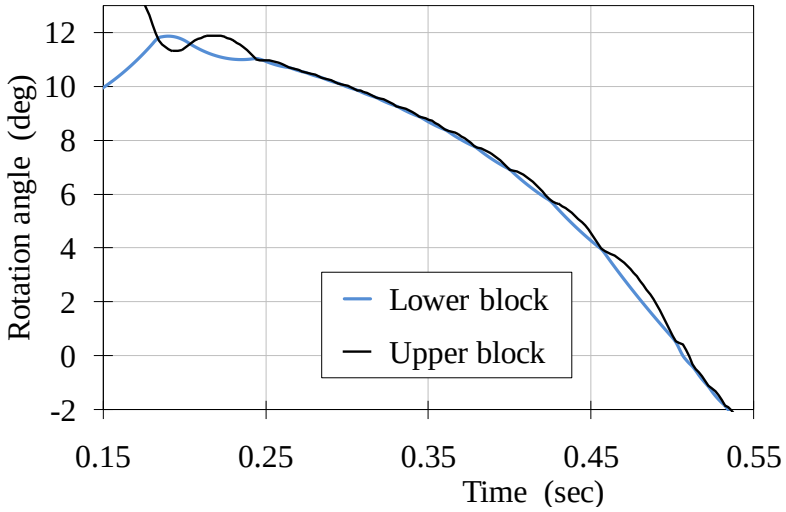

Figure 20: Magnification of rotation angle graph of Figure 15A.

As shown in Figure 17A, the numerical response for a sine acceleration wave of 7 Hz frequency and 3 mm amplitude agrees well with the experimental data, predicting the periodic motion, the amplitude and the phase difference (180 deg) of the two blocks (though the measurements error for the lower block is high due to small angles). Moreover, this motion is established only after a few seconds, in both the laboratory tests and the algorithm results.

In Figure 17B, the numerical response for a sine wave of 5.5 Hz frequency and 3 mm amplitude reproduce well the behaviour observed in the tests for same excitation conditions, namely very small angles of the lower block that eventually remains almost still, while the upper block obtains a periodic motive. Figure 17C shows a similar behaviour but for a quite different combination of excitation frequency and amplitude, 3 Hz and 5 mm.

Finally, in Figure 17D the combination of 4 Hz/3 mm frequency/amplitude of the ground acceleration wave results in a complex non-periodic and non-symmetric response, with the upper block showing much higher vibrations, and with some smaller periods of combined periodic motion of both blocks together. This chaotic response was also observed in the experiments, although not for the same conditions (5 Hz, 5 mm)

The above results confirm the general behaviour of the force-excited two-block system, which was observed both experimentally and numerically, that the two-block system can have numerous different response patterns, periodic or not, and it is very sensitive to excitation conditions. Even a minor change of either the amplitude or the frequency of the external acceleration can cause a completely different rocking motion motive.

5 Conclusion

In this project, the dynamic behaviour during rocking motion of a single and a two rigid blocks system was investigated. The main stages and corresponding objectives of this study were:

- Derivation of a compact mathematical model describing the equations of motion of one & two rocking blocks
- Development of a computer software for numerical simulation of free or forced rocking of a block system
- Construction of a test platform in the laboratory and measure corresponding free and forced motion of rocking blocks

For both single-block and double-block systems the derivation of the mathematical model was divided in two parts: the equations of motion and the equations of impact. The final model can combine all possible relative positioning and motion of up to two blocks, into a single set of analytic expressions, by the introduction of binary indicators (C_R). This is a significant advantage of the present approach compared to the literature that generalize the analysis and facilitate the numerical simulation and the validation of correctness and accuracy of the results.

The analytical expressions were numerically integrated on a specially developed computer program on Matlab. The time step for independent results was found to be 10^{-4} sec and the optimum integration method was the 4^{th} order Runge-Kutta. The algorithm underwent several self-symmetry tests for single and double block rocking cases, in order to ensure that it is perfectly correct. This procedure revealed that the numerical results are very sensitive to even minor modelling or programming errors. The compact mathematical model derived in this report facilitated significantly the debugging task, that otherwise would be extremely laborious.

The results of the numerical algorithm were also validated experimentally for free and forced rocking motion of single and two block systems. Repeatability was confirmed by several sets of measurements for each case, based on which the absolute error of the angle and time measurements was found to be $\pm 0.5^{o}$ and 0.1 sec, respectively. An error estimation method showed that the relative error in the angular acceleration was within ±14%, which is at about the same order of magnitude with other experimental works in the literature, and caused mainly by the sensitivity of the results on the initial and testing conditions.

The coefficient of restitution of the lower block, as obtained by the angular momentum conservation model, had to be corrected in order to match the numerical results with the experiments, in accordance with the findings of other researchers. The correction factor was found to correlate with the aspect ratio of the rocking blocks. The developed model was also used to produce an overturning map for a single block, as an indicative application for realistic problems. However, the rocking motion of a two-block system subjected to an external simple sinus excitation become very complex and can take numerous patterns, depending on the exact initial and testing conditions.

In concluding, this study showed that reliable numerical modelling of the rocking block problem is feasible, but requires experimental data to make the analytic model results applicable for real materials and actual block geometry.

6 References

Aslam, M., Salise, D.T. and Godden, W.G. (1980), "Earthquake Rocking Response of Rigid Bodies", *Journal of the Structural Division, ASCE,* **106** (2), 377-392.

Baratta, A. and Corbi, O. (2012), "Analysis of the Dynamics of Rigid Blocks Using the Theory of Distributions", *Advances in Engineering Software*, **44**, 15-25.

Chapra, S.C. and Canale, R.P. (1998), *Numerical Methods for Engineers*: WCB/McGraw-Hill.

Dimitrakopoulos, E.G. and Dejong, M. (2012), "Revisiting the Rocking Block: Closed-form Solutions and Similarity Laws", *Proceeding of the Royal Society A,* **468**, 2294-2318.

ElGawady, M.A., Ma, G., Butterworth, J. & Ingham, J.M. (2006), Probabilistic Analysis of Rocking Blocks, *2006 New Zealand Society of Earthquake Engineering Conference,* New Zealand.

Housner, G.W. (1963), "The Behavior of Inverted Pendulum Structures during Earthquakes", *Bul-letin of the Seismological Society of America*, **53**, 403-417.

Ishiyama, Y. (1982), "Motions of Rigid Bodies and Criteria for Overturning by Earthquake Excitations", *Earthquake Engineering and Structural Dynamics*, **10**, 635-650.

Kalliontzis, D., Sritharan, S., & Schultz, A.E. (2017), "Improving Accuracy of the Simple Rocking Model of Rigid Blocks, *16th World Conference on Earthquake, 16WCEE 2017,* Santiago, Chile.

Kounadis, A.N., Papadopoulos, G.J., and Cotsovos D.M. (2012), "Overturning Instability of a Two-Rigid Block System Underground Excitation", *Journal of Applied Mathematics and Mechanics,* **92**, 536-557.

Kounadis, A.N. (2013), "Rocking instability of Free-Standing Statues atop Slender Cantilevers Under Ground Motion", *Soil Dynamics and Earthquake Engineering*, **48**, 294-305.

Makris, N. and Vassiliou, M.F. (2015), "The dynamics of the Rocking Frame", in Psycharis, I.N., Pantazopoulou, S. & Papadrakakis M. (eds.), *Seismic Assessment, Behaviour and Retrofit of Heritage Buildings and Monuments, Computational Methods in Applied Sciences* 37, Springer, pp. 37-59.

Minafo, G., Amato, G. and Stella, L. (2016), "Rocking Behaviour of Multi-block Columns Subjected to Pulse-type Ground Motion Accelerations", *The Open Construction and Building Technology Journal*, pp. 150-157.

Mouzakis, H., Psycharis, I., Papastamatiou, D., Carydis, P., Papantonopoulos, C. and Zambas C. (2002), "Experimental Investigation of the Earthquake Response of a Model of a Marble Classical Column", *Earthquake Engineering Structural Dynamics*, **31**, 1681-1698.

Rajasekaran, S. (2009), *Structural Dynamics of Earthquake Engineering*: Woodhead Publishing.

Schau, H. and Johannes, M. (2013), "Rocking and Sliding of Unanchored Bodies Subjected to Seismic Load According to Conventional and Nuclear Rules", *4th ECCOMAS Thematic Conference on Computational Methods in Structural Dynamics and Earthquake Engineering*, Kos Island, Greece.

Spanos, P.D., Roussis, P.C., Politis, P.A. (2001), "Dynamic Analysis of Stacked Rigid Blocks", *Soil Dynamics and Earthquake Engineering*, **21**, 559-578.

Voyagaki, E., Psycharis, I.N. and Mylonakis, G.E. (2012), "Rocking Response and Overturning Criteria for free Standing Blocks to Single-lobe Pulses", *15th World Conference on Earthquake Engineering*, Lisboa, Portugal.

http://www.steelconstruction.info/Modular_construction

https://triumphmodular.com/wp-content/uploads/2014/09/MBI_Durability_Paper.pdf

7 Appendix

Displacements with respect to the lower left corner

$$u_{LL} = 2hsin(\theta) \tag{A1}$$

$$v_{LL} = 2R(\cos(a) - 1) \tag{A2}$$

$$u_{RL} = -2Rcos(a)\sin(\theta) \tag{A3}$$

$$v_{RL} = 2R[sin(a) - \sin(\alpha + \theta)] \tag{A4}$$

$$u_{CL} = \frac{u_{RL}}{2}, \quad v_{CR} = \frac{v_{RL}}{2} \tag{A5}$$

Differential terms for Euler-Lagrange equation

$$\frac{du_{T1}}{d\theta_1} = R_1[C_{R1}\cos(a_1 - \theta_1) + (1 - C_{R1})\cos(a_1 + \theta_1)] \tag{A6}$$

$$\frac{dv_{T1}}{d\theta_1} = R_1[C_{R1}\sin(a_1 - \theta_1) - (1 - C_{R1})\sin(a_1 + \theta_1)] \tag{A7}$$

$$\frac{du_{T2}}{d\theta_2} = R_2[C_{R2}\cos(a_2 - \theta_2) + (1 - C_{R2})\cos(a_2 + \theta_2)] \tag{A8}$$

$$\frac{dv_{T2}}{d\theta_2} = R_2[C_{R2}\sin(a_2 - \theta_2) - (1 - C_{R2})\sin(a_2 + \theta_2)] \tag{A9}$$

$$\frac{du_{T2}}{d\theta_1} = 2h_1\cos(\theta_1)(1 - |C_{R1} - C_{R2}|) + 2R_1|C_{R1} - C_{R2}|[\cos(\alpha_1 - \theta_1)\,C_{R1} + + \cos(\alpha_1 - \theta_1)\,C_{R2}] \tag{A10}$$

$$\frac{dv_{T2}}{d\theta_1} = -2h_1\sin(\theta_1)(1 - |C_{R1} - C_{R2}|) + 2R_1|C_{R1} - C_{R2}|[\sin(\alpha_1 - \theta_1)\,C_{R1} - - \sin(\alpha_1 - \theta_1)\,C_{R2}] \tag{A11}$$

$$\frac{du_{T1}}{d\theta_2} = 0 \tag{A12}$$

$$\frac{dv_{T1}}{d\theta_2} = 0 \tag{A13}$$

Coefficients of the linear equations system (32) for impacts between block 1 and ground

$$A_1 = 2m_2R_2F^+ \tag{A14}$$

$$B_1 = I_2 + m_2R_2^2 \tag{A15}$$

$$C_1 = (I_2 + m_2R_2^2)\dot{\theta}_2^- + 2m_2R_2F^-\dot{\theta}_1^- \tag{A16}$$

$$A_2 = I_1 + m_1R_1^2 + m_2d_1\big(Ecos(\varphi_1) - Zsin(\varphi_1)\big) \tag{A17}$$

$$B_2 = I_2 + m_2d_1(Acos(\varphi_1) - Bsin(\varphi_1)) \tag{A17}$$

$$C_2 = m_2 d_1\left(C\dot{\theta}_1^- \cos(\varphi_1) + A\dot{\theta}_2^- \cos(\varphi_1) - D\dot{\theta}_1^- \sin(\varphi_1) - B\dot{\theta}_2^- \sin(\varphi_1)\right) +$$
$$+I_2\dot{\theta}_2^- + (I_1\dot{\theta}_1^- + m_1 R_1^2 \cos(2a_1))\,\dot{\theta}_1^- \quad \text{(A18)}$$

where

$$A = R_2[cos(a_2 - \theta_2)C_{R2} + cos(a_2 + \theta_2)(1 - C_{R2})] \quad \text{(A19)}$$

$$B = R_2[sin(a_2 - \theta_2)C_{R2} - sin(a_2 + \theta_2)(1 - C_{R2})] \quad \text{(A20)}$$

$$C = 2h_1(2C_{R1}C_{R2} + 1 - C_{R1} - C_{R2}) + 2R_1 cos(a_1)(C_{R1} + C_{R2} - 2C_{R1}C_{R2}) \quad \text{(A21)}$$

$$D = 2R_1 sin(a_1)(C_{R1} - C_{R2}) \quad \text{(A22)}$$

$$E = 2h_1[2(1 - C_{R1})C_{R2} + C_{R1} - C_{R2}] + 2R_1 cos(a_1)[(1 - C_{R1})(1 - 2C_{R2}) + C_{R2}] \quad \text{(A23)}$$

$$Z = 2R_1 sin(a_1)[(1 - C_{R1}) - C_{R2}] \quad \text{(A24)}$$

$$F^+ = h_1 cos(a_2 - C_{Z2}\theta_2)|C_{R1} - C_{R2}| + R_1 cos(a_1 + a_2 - C_{Z2}\theta_2)(1 - |C_{R1} - C_{R2}|) \quad \text{(A25)}$$

$$F^- = h_1 cos(a_2 - C_{Z2}\theta_2)(1 - |C_{R1} - C_{R2}|) + R_1 cos(a_1 + a_2 - C_{Z2}\theta_2)|C_{R1} - C_{R2}| \quad \text{(A26)}$$

$$\varphi_1 = \text{atan}\left(\frac{C_{Z1}l_2 + u_{c2}}{2h_1 + h_2 + v_{c2}}\right) \quad \text{(A27)}$$

$$d_1 = \sqrt{(2h_1 + h_2 + v_{c2})^2 + (C_{Z1}l_2 + u_{c2})^2} \quad \text{(A28)}$$

$$C_{Zi} = \begin{cases} 1, & rotation\ around\ right\ corner \\ -1, & rotation\ around\ left\ corner \end{cases} \quad \text{(A29)}$$

Coefficients of the linear equations system (32) for impacts between block 1 and 2

$$A_1 = 2m_2 R_2 F^+ \quad \text{(A30)}$$

$$B_1 = I_2 + m_2 R_2^2 \quad \text{(A31)}$$

$$C_1 = [I_2 + m_2 R_2^2 \cos(2a_2)]\dot{\theta}_2^- + 2m_2 R_2 F^- \dot{\theta}_1^- \quad \text{(A32)}$$

$$A_2 = I_1 + m_1 R_1^2 + m_2 d_2\left(Ecos(\varphi_2) - Zsin(\varphi_2)\right) \quad \text{(A33)}$$

$$B_2 = I_2 + m_2 d_2(Gcos(\varphi_2) - Hsin(\varphi_2)) \quad \text{(A34)}$$

$$C_2 = m_2 d_2\left(C\dot{\theta}_1^- \cos(\varphi_2) + A\dot{\theta}_2^- \cos(\varphi_2) - D\dot{\theta}_1^- \sin(\varphi_2) - B\dot{\theta}_2^- \sin(\varphi_2)\right) +$$
$$+I_2\dot{\theta}_2^- + I_1\dot{\theta}_1^- + m_1 R_1^2\dot{\theta}_1^- \quad \text{(A35)}$$

where

$$A = R_2[cos(a_2 - \theta_2)C_{R2} + cos(a_2 + \theta_2)(1 - C_{R2})] \quad \text{(A36)}$$

$$B = R_2[sin(a_2 - \theta_2)C_{R2} - sin(a_2 + \theta_2)(1 - C_{R2})] \quad \text{(A37)}$$

$$C = [2h_1 cos(\theta_1)(2C_{R1}C_{R2} + 1 - C_{R1} - C_{R2})] + 2R_1[cos(a_1 - \theta_1)C_{R1}(1 - C_{R2})$$
$$+cos(a_1 + \theta_1)C_{R2}(1 - C_{R1})] \quad \text{(A38)}$$

$$D = [-2h_1 sin(\theta_1)(2C_{R1}C_{R2} + 1 - C_{R1} - C_{R2})] + 2R_1[sin(a_1 - \theta_1)C_{R1}(1 - C_{R2})$$

$$-sin(a_1+\theta_1)C_{R2}(1-C_{R1})] \quad \text{(A39)}$$

$$E = [2h_1cos(\theta_1)(2(1-C_{R2})C_{R1}+1-(1-C_{R2})-C_{R1})] + 2R_1[cos(a_1-\theta_1)C_{R1}C_{R2}$$
$$+cos(a_1+\theta_1)(1-C_{R2})(1-C_{R1})] \quad \text{(A40)}$$

$$Z = [-2h_1sin(\theta_1)(2(1-C_{R2})CR_1+1-(1-C_{R2})-C_{R1})] + 2R_1[sin(a_1-\theta_1)C_{R1}C_{R2}$$
$$-sin(a_1+\theta_1)(1-C_{R2})(1-C_{R1})] \quad \text{(A41)}$$

$$F^+ = R_1cos(a_1+a_2)(1-|C_{R1}-C_{R2}|)+h_1cos(a_2)|C_{R1}-C_{R2}| \quad \text{(A42)}$$

$$F^- = F^+ \quad \text{(A43)}$$

$$G = R_2[cos(a_2-\theta_2)(1-C_{R2})+cos(a_2+\theta_2)C_{R2}] \quad \text{(A44)}$$

$$H = R_2[sin(a_2-\theta_2)(1-C_{R2})-sin(a_2+\theta_2)C_{R2}] \quad \text{(A45)}$$

$$\varphi_2 = \theta_1 - \text{atan}\left(\frac{C_{Zi}l_2}{2h_1+h_2}\right) \quad \text{(A46)}$$

where $l_i = b_i$ (A47)